Interannual Variability in the Southern Hemisphere Circulation Organized by Stratospheric Final Warming Events

Robert X. Black
Brent A. McDaniel
School of Earth and Atmospheric Sciences
Georgia Institute of Technology
Atlanta, Georgia

September 2006
(To appear in the *Journal of the Atmospheric Sciences:*
Special Issue on Annular Modes and Jets)

Corresponding author address:
Dr. Robert X. Black
School of Earth and Atmospheric Sciences
Georgia Institute of Technology
Atlanta, GA 30332-0340
E-mail: rob.black@eas.gatech.edu

ABSTRACT

A composite observational analysis is presented demonstrating that austral stratospheric final warming (SFW) events provide a substantial organizing influence upon the large-scale atmospheric circulation in the Southern Hemisphere. In particular, the annual weakening of high latitude westerlies in the upper troposphere and stratosphere is accelerated during SFW onset. This behavior is associated with a coherent annular circulation change with zonal wind decelerations (accelerations) at high (low) latitudes. The high latitude stratospheric decelerations are induced by the anomalous wave driving of upward propagating tropospheric waves. Longitudinally asymmetric circulation changes occur in the lower troposphere during SFW onset with regionally localized height increases (decreases) at subpolar (middle) latitudes. Importantly, the tropospheric and stratospheric circulation change patterns identified here are structurally distinct from the Southern Annular Mode. It is concluded that SFW events are linked to interannual atmospheric variability with potential bearing upon weather and climate prediction.

1. Introduction

There is increasing observational evidence linking the strength of the winter stratospheric polar vortex to tropospheric climate via circumpolar annular modes (Thompson and Wallace 2000, Baldwin and Dunkerton 2001, Thompson et al. 2005). The general association found is that a strengthened stratospheric polar vortex is typically associated with intensified tropospheric westerlies near 55^{o}N and vice-versa. As a consequence, annular modes also act to modulate tropospheric weather (Thompson and Wallace 2001, Baldwin et al. 2003). These annular modes occur in both the Northern and Southern Hemispheres (denoted NAM and SAM, respectively) and over a wide range of time scales (weeks to decades). Most recent research examining connections between the stratospheric polar vortex and tropospheric circulation patterns has focused on either subseasonal variability (e.g., Limpasuvan et al. 2004, McDaniel and Black 2005) or long-term trends (Thompson and Solomon 2002, Gillett and Thompson 2003).

The stratospheric polar vortex is characterized by an annual cycle that terminates with a relatively rapid breakdown known as the stratospheric final warming (or SFW), which typically occurs during spring. However, considerable interannual variability in the timing of SFW events is observed (e.g., Waugh and Rong 2002) since they are initiated by transient Rossby wave packets propagating upward from tropospheric altitudes. This raises the intriguing scientific question of whether SFW events provide an organizing influence on the stratosphere-troposphere circulation akin to the annular mode behavior described above. For example, are early polar vortex breakdowns accompanied by parallel anomalous weakenings in the tropospheric westerlies near 55^{o}N? The existence of such behavior will have a particular bearing upon the understanding, simulation, and prediction of extratropical seasonal transitions as well as interannual circulation variability.

A recent observational analysis of the Northern Hemisphere circulation indicates that, in fact, Northern Hemisphere SFW events accelerate the seasonal weakening of high latitude circumpolar westerlies (in contrast to the climatological trend) simultaneously in the stratosphere and troposphere (Black et al. 2006, BMR hereafter). The time evolution of the SFW events consists of a bi-directional dynamical coupling in which tropospheric planetary waves weaken the stratospheric polar vortex followed by weakened westerlies in the upper troposphere, as for the NAM. However, a closer inspection reveals that the tropospheric manifestation of Northern Hemisphere SFW events are patterns that only qualitatively resemble the canonical NAM pattern as the respective anomaly centers are retracted poleward in the former.

We study the important analogous problem of how SFW events in the Southern Hemisphere organize the large-scale circulation of the stratosphere and troposphere. The current work is distinct from other recent studies of individual cases (Orsolini et al. 2005), month-to-month variability (Hio and Yoden 2005), or subseasonal SAM events (Thompson et al. 2005) in that we perform a daily resolution composite analysis keyed onto the final weakening of the polar vortex (these three papers are part of a collection emphasizing the unusual behavior of the Southern Hemisphere atmospheric circulations during 2002, which was marked by a unique subseasonal stratospheric warming event in September). Our analysis makes no a priori assumptions regarding the structural evolution of the organized response as the data are not projected upon predetermined modes of variability (such as the SAM). In fact, the distinctions between SFW-associated variability and SAM structures represent a key result of the paper.

2. Data and Methods

The basic input data for our study are the ERA-40 daily-average reanalyses (Kallberg et al. 2004) archived on 21 pressure levels extending from 1000 hPa to 1 hPa. We study the characteristics of 24 SFW events occurring during the satellite era of the ERA-40 data record (1978-2001). Thus our analysis implicitly excludes information on the outlier 2002 season discussed above. Following BMR, we are interested in constructing composites relative to the time when SFW events emerge in the lower stratosphere (at which time tropospheric linkages are expected to be maximized). To this end, SFW events are identified as the final time that the zonal-mean zonal wind at 60°S (the core of the polar vortex in the lower stratosphere) drops below 10 m/s until the subsequent autumn[1]. We apply this criterion to running 5-day averages at 50 hPa. Circulation anomalies are defined as deviations from a smoothed climatological trend (defined as the sum of the first 6 Fourier harmonics of a seasonal cycle derived from an annual time-series of long-term daily averages). The statistical significance of the composite anomalies is assessed using a Student t-test (each annual SFW event is considered an independent sample). The SFW dates identified are used to construct lag composite time evolutions using the 24 years considered (1978-2001). The structural evolution is contrasted with canonical SAM patterns and parallel SFW analyses for the Northern Hemisphere. Quantitative comparisons with SAM are obtained by calculating spatial pattern correlations (from 20°S to 90°S) between the current SFW patterns and the corresponding SAM patterns for November-December

[1] Although the zonal winds in the middle and upper stratosphere become markedly easterly during austral summer, the zonal winds near 50 mb asymptote toward zero (e.g., Fig. 2).

(the time period during which SFW events occur).[2]

3. Results

A time series of the individual onset dates are displayed in Fig. 1 along with a least-squares fit to the time series. The onset dates range from November 14 (1978) to January 3 (1999/2000) with a mean date of December 4 and a standard deviation of 13 days. Thus, all of the events occur well after the "weak" subseasonal SAM events studied by Thompson et al. (2005). We note two features of particular interest in Fig. 1. First there is statistically significant trend[3] of +1.09 days per year in the annual timing of Southern Hemispheric SFW events. The increasing trend is in accord with the results of Waugh et al. (1999) and is physically consistent with Thompson and Solomon (2002), who observed a long term strengthening in the southern hemisphere stratospheric polar vortex during the November-December time frame. A second interesting feature in Fig. 1 is the general increase in the level of interannual variability that occurs between the early and latter portions of the data record. This appears counter to what one would expect in association with a stronger and more persistent polar vortex.

A lag composite analysis of the evolution of the zonal-average zonal wind at high latitudes is presented in Fig. 2 along with the corresponding climatological trend. The wind is averaged over

---

[2] The SAM patterns are calculated via linear regressions with the SAM indices obtained from the NOAA Climate Prediction Center at http://www.cpc.noaa.gov/products/precip/CWlink/.

[3] The trend is statistically significant from zero at the 99% confidence level according to the t-statistic.

a latitudinal band (60°S to 70°S) that simultaneously encompasses strong zonal wind tendencies in the both the troposphere an stratosphere (see Fig. 3). The composite evolution is centered on lag 0 (relative to SFW onset) while the climatological trend is centered on the mean SFW onset date (Dec. 4). In both cases the evolution is characterized by (a) a transition towards easterly winds in the mid to upper stratosphere and (b) a weakening of the westerlies in the upper troposphere and lower stratosphere. However, it is also evident that both of these tendencies are more strongly concentrated near day 0 in the SFW composite analysis (note the distinct kinks in the zonal wind contours near day 0). This indicates that SFW events provide an organizing influence which acts to accelerate the large-scale seasonal circulation transition during the brief time period surrounding SFW onset. This behavior is associated with anomalously strong (weak) westerlies in the lower stratosphere prior to (after) Day 0. The strength of this organizational behavior is less pronounced for Southern Hemispheric SFW events than for Northern Hemisphere events (BMR, Fig. 2).

The corresponding time evolution of zonal-mean circulation anomalies is presented in Fig. 3. Significant westerly wind anomalies are observed in the lower stratosphere during the period prior to Day 0 while easterlies anomalies extend throughout much of the stratosphere after Day 0. Unlike for the Northern Hemisphere, however, only marginally significant anomaly signatures are found at tropospheric altitudes (BMR, Fig. 4). On the other hand, an analysis of high latitude Eliassen-Palm fluxes and local wave driving (upper right panel) indicates that tropospheric wave features play a key role in enacting the SFW events. There is an anomalous upwards burst of Eliassen-Palm flux within the troposphere at Day -5. This is connected to the generation of planetary wave activity in the lower stratosphere prior to Day 0 and the stratospheric zonal wind deceleration occuring during SFW onset. This behavior bears a strong resemblance to Northern Hemisphere SFW events (BMR).

Most of the zonal decelerations occurring in association with SFW events are complete by Day +5. The net zonal wind change occurring during the period prior to Day +5 is displayed in the bottom of Fig. 3. At stratospheric altitudes there is a north-south dipole consisting of significant decelerations (accelerations) poleward (equatorward) of 50°S. Although these change patterns extend downward into the troposphere, only the tropospheric decelerations at high latitudes are statistically significant. Although the high latitude deceleration pattern tilts poleward with height (similar to the canonical SAM pattern), both the stratospheric and tropospheric latitudinal minima are phase-shifted compared to corresponding SAM features (Fig 7a of Thompson and Wallace 2000, noting that their figure only extends to 50 hPa). In particular, the stratospheric deceleration maximum is shifted 10° southward and 30 hPa upward relative to the corresponding SAM feature. Meanwhile, the low latitude (35°S) acceleration feature in Fig. 3 attains peak amplitudes in the middle stratosphere (near 25 hPa) unlike the SAM feature, which peaks in the upper troposphere (near 250 hPa). This lack of correspondence is quantitatively confirmed via a spatial pattern correlation analysis, which reveals that the SFW zonal wind change pattern (in Fig. 3) shares a common spatial variability ($100\rho^2$) of only 38% with the canonical SAM pattern. The results imply that, although SFW events are clearly associated with annular circulation changes, these patterns have important distinctions from SAM. An implication is that observational studies focusing solely on SAM variability will likely incorrectly capture annular variability associated with SFW events which, at the very least, appear to involve ancillary annular circulation structures.

We next examine the near-surface geopotential signature, or "footprint", of SFW events. The relative lack of strong tropospheric signatures in the previous zonal-mean analyses might lead one to expect little or no signature in the lower troposphere. However, regionally localized patterns

remain possible as they would be substantially weakened or removed upon zonal averaging. Fig. 4 contrasts the 850 hPa composite anomaly field for respective early and late stages of the SFW time evolution (The 850 hPa level is chosen instead of 1000 hPa to minimize the impact of vertical interpolation below the surface of Antarctica). These patterns can be qualitatively compared to the SAM pattern in Fig. 5a of Thompson and Wallace (2000 - noting that their polar stereographic map is rotated by 90^{o} longitude with respect to ours). Five day averages are performed to isolate the slowly varying component of the tropospheric circulation (minimizing noise due to baroclinic wave activity) In addition to applying point-wise t-tests, the field significance of the anomaly patterns displayed in Fig. 4 was tested using the methodology of Livezey and Chen (1983).[4]

We first note that the anomaly patterns in Fig. 4 generally exhibit much more longitudinal asymmetry than observed for SAM. Concentrating on the statistically significant features, the early stages of the evolution are characterized by anomalously low heights over the Antarctic Peninsula and the Weddell Sea with positive midlatitude anomalies concentrated within three localized centers. During SFW onset these features are replaced by a pattern of weakly significant positive anomalies over eastern Antarctica. The corresponding height change field consists of significant height increases localized over portions of Antarctica (with a strong projection on wavenumber 2) and a

[4] In each case a Monte Carlo resampling of the input anomaly fields was performed by randomly sampling SFW onset dates from an observationally constrained gaussian distribution. These dates were then used to construct 1000 synthetic composite fields, the distribution of which places statistical bounds on the fractional areal coverage by significant anomalies that would be expected to occur by chance.

wavenumber 3 pattern of midlatitude height decreases. The zonal mean of this pattern is dynamically consistent with the earlier noted zonal-mean tropospheric decelerations located between 60°S and 70°S (Fig. 3). Both the precursor anomaly pattern and the anomaly change pattern are field significant at the 95% confidence level. The change pattern primarily represents the elimination of the precursor anomaly structure. The initial anomaly pattern is consistent with the existence of enhanced tropospheric planetary wave activity prior to SFW onset. As found in the zonal-mean analyses, the surface height change pattern has clear distinctions from the canonical SAM pattern, the latter of which has much greater longitudinal symmetry with the strongest geopotential gradients located equatorward of Antarctica (Thompson and Wallace 2000, Fig. 5a). Spatial pattern correlation analysis quantitatively verifies these distinctions, as each anomaly pattern in Fig. 4 shares a common spatial variability with the canonical SAM of 30% or less. The composite analyses show that the tropospheric circulation evolution during SFW events has considerable longitudinal structure that is not well represented in terms of annular modes (SAM or otherwise). This is a different result than found for Northern Hemisphere SFW events (BMR), in which case tropospheric annular structures are simply retracted poleward in comparison to NAM structures.

4. Summary

A composite observational analysis has been performed to study the extent to which Southern Hemisphere stratospheric final warming (SFW) events provide an organizing influence on the large-scale circulation of the stratosphere and troposphere. We find that SFW events act to concentrate part of the annual weakening of the high latitude circumpolar westerlies in the uppermost troposphere and stratosphere to occur within a relatively brief time period surrounding

SFW onset. This behavior is associated with zonal-mean westerly (easterly) anomalies in the lower stratosphere prior to (after) SFW onset. A coherent annular circulation change occurs during SFW onset with zonal decelerations (accelerations) observed at high (low) latitudes. However, this annular pattern is (a) relatively weak at tropospheric altitudes and (b) structurally distinct from the subseasonal SAM structure identified by Thompson and Wallace (2000). The latter behavior is also observed in association with Northern Hemisphere SFW events (BMR). The high latitude stratospheric decelerations are induced by anomalous wave driving associated with upward propagating tropospheric waves at high latitudes.

The structural distinctions with the SAM are somewhat surprising given the result of Baldwin et al. (2003) that tropospheric SAM *persistence* is maximized during the November-December time frame. However, Baldwin et al. also demonstrate that tropospheric SAM *variance* is maximized during July and drops markedly between September and November (see their Fig. 1). One possibility is that, even though a weak (strong) polar vortex in the Southern Hemisphere favors the occurrence of negative (positive) tropospheric SAM events, the short time scale weakening (or strengthening) of the polar vortex may be associated with tropospheric circulation features (annular or otherwise) that are distinct from the SAM. This suggests that one must be cautious in implicitly phrasing large-scale atmospheric behavior solely in terms of predefined modes of variability (e.g., see below).

The relative weakness of the tropospheric annular structures is quite different than found in the Northern Hemisphere. This may simply reflect the enhanced vigor of Northern Hemisphere SFW events which tap upon a greater reservoir of tropospheric planetary wave activity. Nonetheless, we

do observe significant lower tropospheric circulation changes in association with SFW onset. The circulation change pattern is longitudinally asymmetric with regionally localized height increases (decreases) observed at subpolar (middle) latitudes, lacking the annular structure of the SAM.

We conclude that SFW events provide a substantial organizing influence upon the large-scale circulation of the southern hemisphere. Consequently, SFW events provide a potentially important source of interannual variability since the annual timing of SFW events is highly variable. We further conclude that SFW events are associated with annular variability that is distinct from the canonical annular mode structures characterized by Thompson and Wallace (2000). An important consequence is that the circulation variability associated with SFW events will be inadequately represented by annular mode measures such as multilevel SAM indices. We speculate that interannual atmospheric circulation variability associated with SFW events may have a practical bearing upon weather and climate prediction.

Acknowledgments

The study is supported by the NSF Climate and Large-Scale Dynamics Program under Grant ATM-0456157 (under the U.S. CLIVAR Program) and NASA's Living With a Star Targeted Research and Technology Program under Grant NAG5-13492. The ERA-40 data are provided by ECMWF via NCAR's Data Support Section.

References

Baldwin, M. P., and T. J. Dunkerton, 2001: Stratospheric harbingers of anomalous weather regimes. *Science*, **294,** 581-584.

Baldwin, M. P., D. B. Stephenson, D. W. J. Thompson, T. J. Dunkerton, A. J. Charlton, and A. O'Neill, 2003: Stratospheric memory and skill of extended-range weather forecasts. *Science*, **301,** 636-640.

Black, R. X., B. A. McDaniel, and W. A. Robinson, 2006: Stratosphere-Troposphere coupling during spring onset. *J. Climate,* **19,** 4891-4901. Preprint available at: http://rxb.eas.gatech.edu/papers/black_mcdaniel_robinson.pdf

Gillett, N. P., and D. W. J. Thompson, 2003: Simulation of recent Southern Hemisphere climate change. *Science*, **302,** 273-275.

Hio, Y., and S. Yoden, 2005: Interannual variations of the seasonal march in the Southern Hemisphere stratosphere for 1979-2002 and characterization of the unprecedented year 2002. *J. Atmos. Sci.,* **62,** 567-579.

Kallberg, P., A. Simmons, S. Uppala, and M. Fuentes, 2004: The ERA-40 archive, *ERA-40 Project Report Series 17*, European Centre for Medium-range Weather Forecasts, Reading, UK.

Limpasuvan, V., D. W. J. Thompson, and D. L. Hartmann, 2004: On the life cycle of Northern Hemisphere stratospheric sudden warmings. *J. Climate*, **17,** 2584-2596.

McDaniel, B.A., and R.X. Black, 2005: Intraseasonal dynamical evolution of the Northern Annular Mode. *J. Climate,* **18,** 3820-3839.

Orsolini, Y. J., C. E. Randall, G. L. Manney, and D. R. Allen, 2005: An observational study of the final breakdown of the Southern Hemisphere stratospheric vortex in 2002. *J. Atmos. Sci.,* **62,** 735-747.

Thompson, D. W. J., and S. Solomon, 2001: Interpretation of recent Southern Hemisphere climate change. *Science,* **296,** 895-899.

Thompson, D. W. J., and J. M. Wallace, 2000: Annular modes in the extratropical circulation Part I: Month- to-month variability. *J. Climate,* **13,** 1000-1016.

Thompson, D. W. J., and J. M. Wallace, 2001: Regional climate impacts of the Northern Hemisphere annular mode. *Science,* **293,** 85-89.

Thompson, D. W. J., M. P. Baldwin, and S. Solomon, 2005: Stratosphere-Troposphere coupling in the Southern Hemisphere. *J. Atmos. Sci.,* **62,** 708-747.

Waugh, D. W., W. J. Randel, S. Pawson, P. A. Newman, E. R. Nash, 1999. Persistence of the lower stratospheric polar vortices, *J. Geophys. Res.*, **104,** 27191-27202.

Waugh, D. W., and P. P. Rong, 2002: Interannual variability in the decay of lower stratospheric Arctic vortices. *J. Meteor. Soc. Japan,* **80,** 997-1012.

Figure Legends

Figure 1. Time series of the annual timing of SFW events at 50 hPa in the Southern Hemisphere (see text for definition details). The blue line depicts the annual timing while the black line represents the long-term trend (least-squares fit) in the time series. The trend line has a slope of 1.09 days/year and is statistically significant from 0 at the 99% confidence level.

Figure 2. The daily time evolution of zonal-mean zonal wind (m s^{-1}) averaged from 60S to 70S. **Left:** The climatological-mean time evolution centered on December 4 (the mean date of SFW events - denoted Lag 0), **Right**: The parallel time evolution for a composite constructed with respect to the annual timing of SFW events at 50 hPa (Lag 0). The contour interval is 2 m s^{-1}.

Figure 3. Anomalies composited with respect to SFW events (Lag 0). Blue and yellow contours denote the 90 and 95% confidence levels for a 2-sided t-test. **Top Left:** Time evolution of composite zonal-mean zonal wind averaged from 60S to 70S (black contours/color shading; units of m s^{-1}). **Top Right**: Time evolution of local wave driving (black contours/color shading; units of m s^{-1} day^{-1}) and red contours indicating regions of upward Eliassen-Palm flux anomalies (units: 10^5 m^3 s^2; contour interval of 0.5) averaged from 50S to 90S. **Bottom Left**: Composite change in the zonal-mean zonal wind anomaly field between lags -20 and +5 (black contours/color shading; units of m s^{-1}).

Figure 4. The 850 hPa geopotential height anomalies (black contours/color shading; units of m) composited with respect to SFW events (Lag 0). Blue and yellow colored contours denote the 90 and 95% confidence levels for a 2-sided t-test. **Top Left:** The time average for lags -20 to -15. **Top Right**: The time average for lags +5 to +10. **Bottom Left**: The difference between the two previous fields. The contour interval is 5 m.

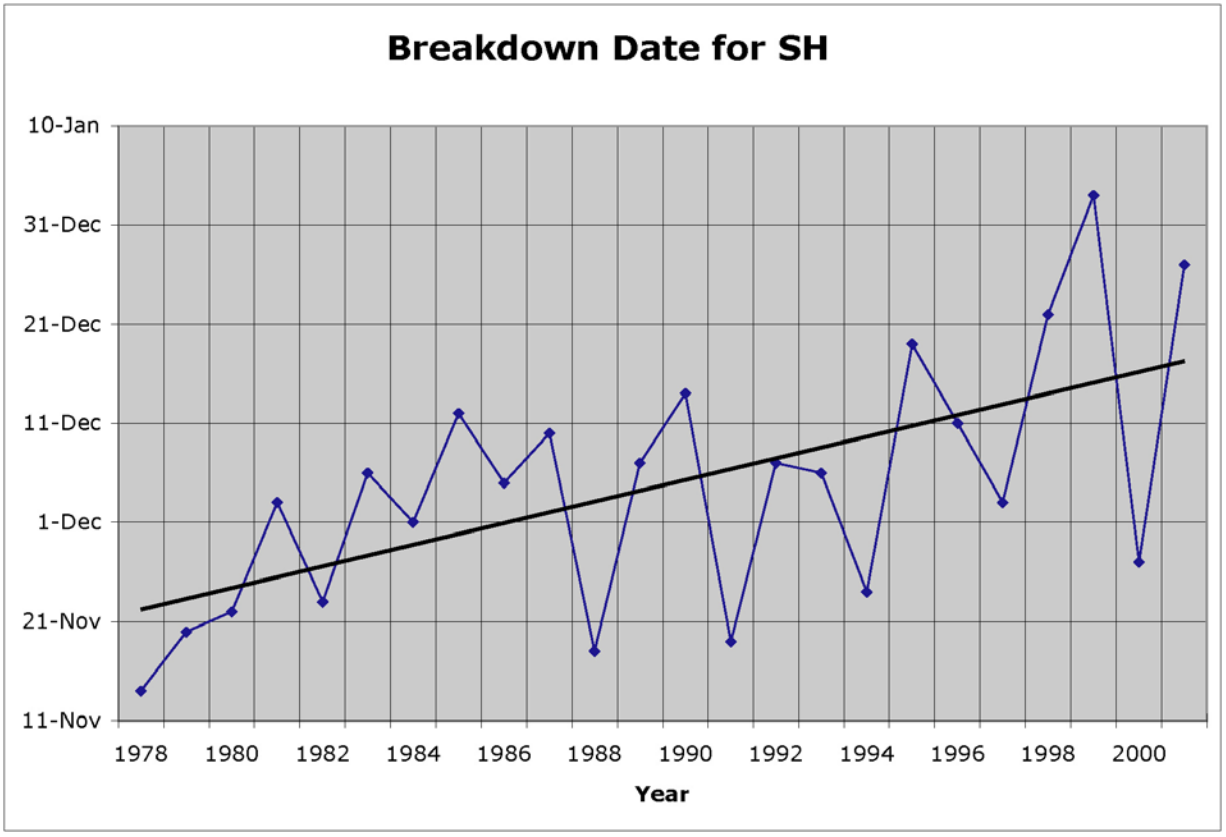

Figure 1

Figure 1. Time series of the annual timing of SFW events at 50 hPa in the Southern Hemisphere (see text for definition details). The blue line depicts the annual timing while the black line represents the long-term trend (least-squares fit) in the time series. The trend line has a slope of 1.09 days/year and is statistically significant from 0 at the 99% confidence level.

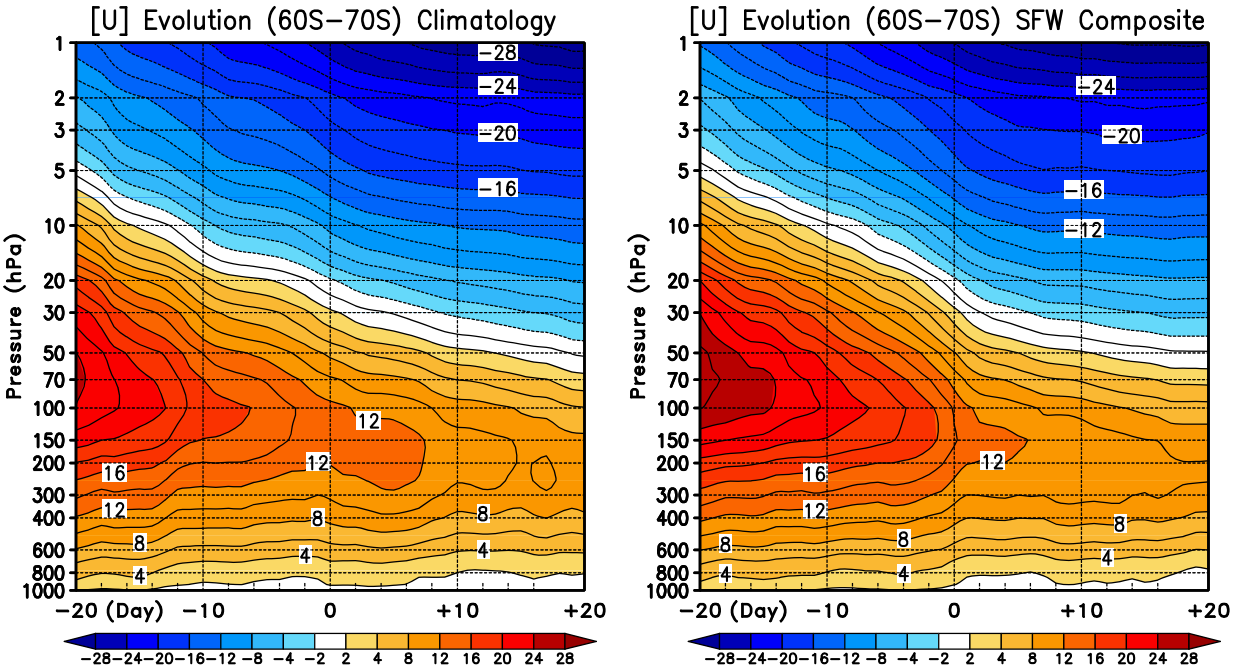

Figure 2

Figure 2. The daily time evolution of zonal-mean zonal wind (m s^{-1}) averaged from 60S to 70S. **Left:** The climatological-mean time evolution centered on December 4 (the mean date of SFW events - denoted Lag 0), **Right**: The parallel time evolution for a composite constructed with respect to the annual timing of SFW events at 50 hPa (Lag 0). The contour interval is 2 m s^{-1}.

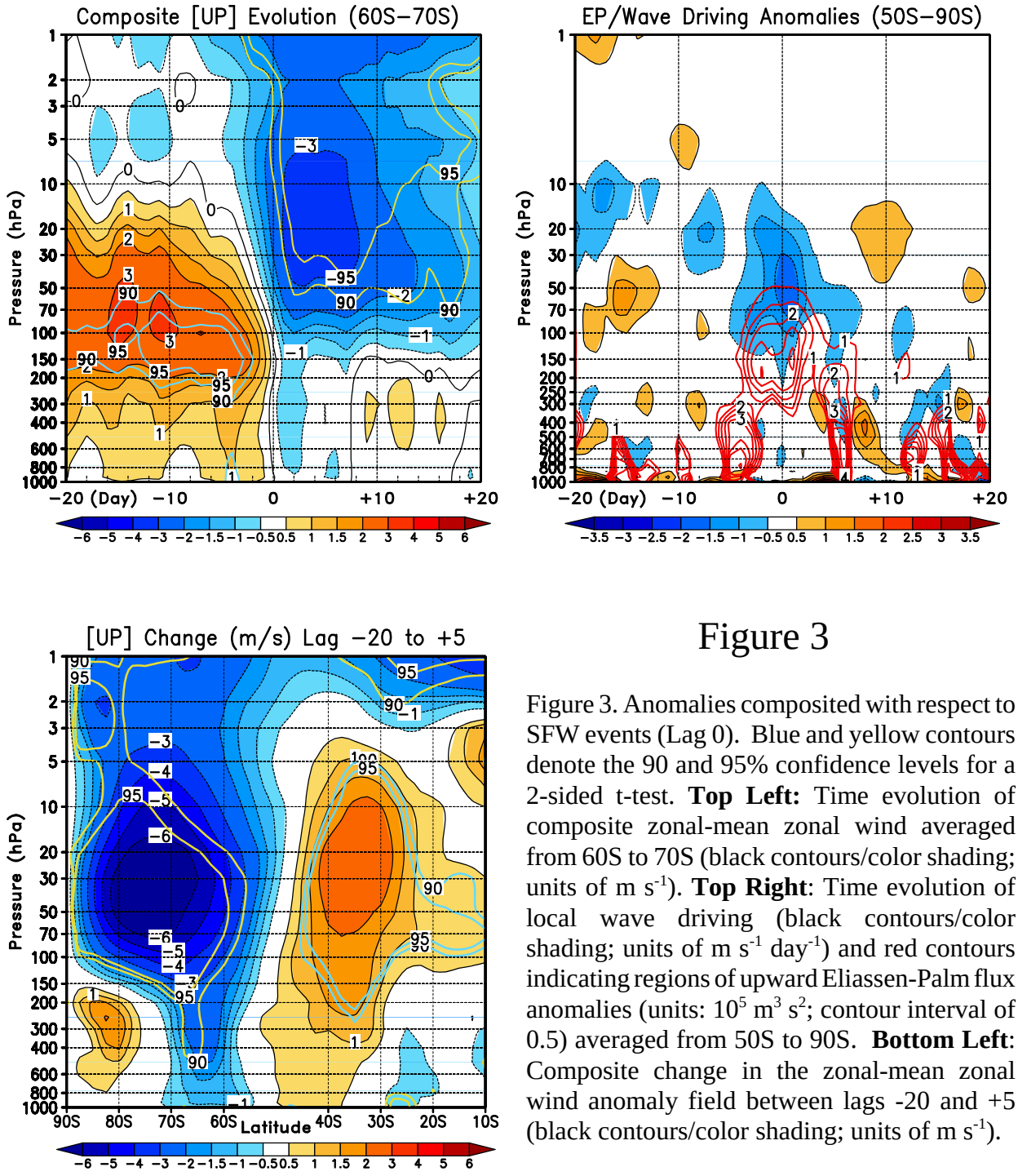

Figure 3

Figure 3. Anomalies composited with respect to SFW events (Lag 0). Blue and yellow contours denote the 90 and 95% confidence levels for a 2-sided t-test. **Top Left:** Time evolution of composite zonal-mean zonal wind averaged from 60S to 70S (black contours/color shading; units of m s^{-1}). **Top Right**: Time evolution of local wave driving (black contours/color shading; units of m s^{-1} day^{-1}) and red contours indicating regions of upward Eliassen-Palm flux anomalies (units: 10^5 m^3 s^2; contour interval of 0.5) averaged from 50S to 90S. **Bottom Left**: Composite change in the zonal-mean zonal wind anomaly field between lags -20 and +5 (black contours/color shading; units of m s^{-1}).

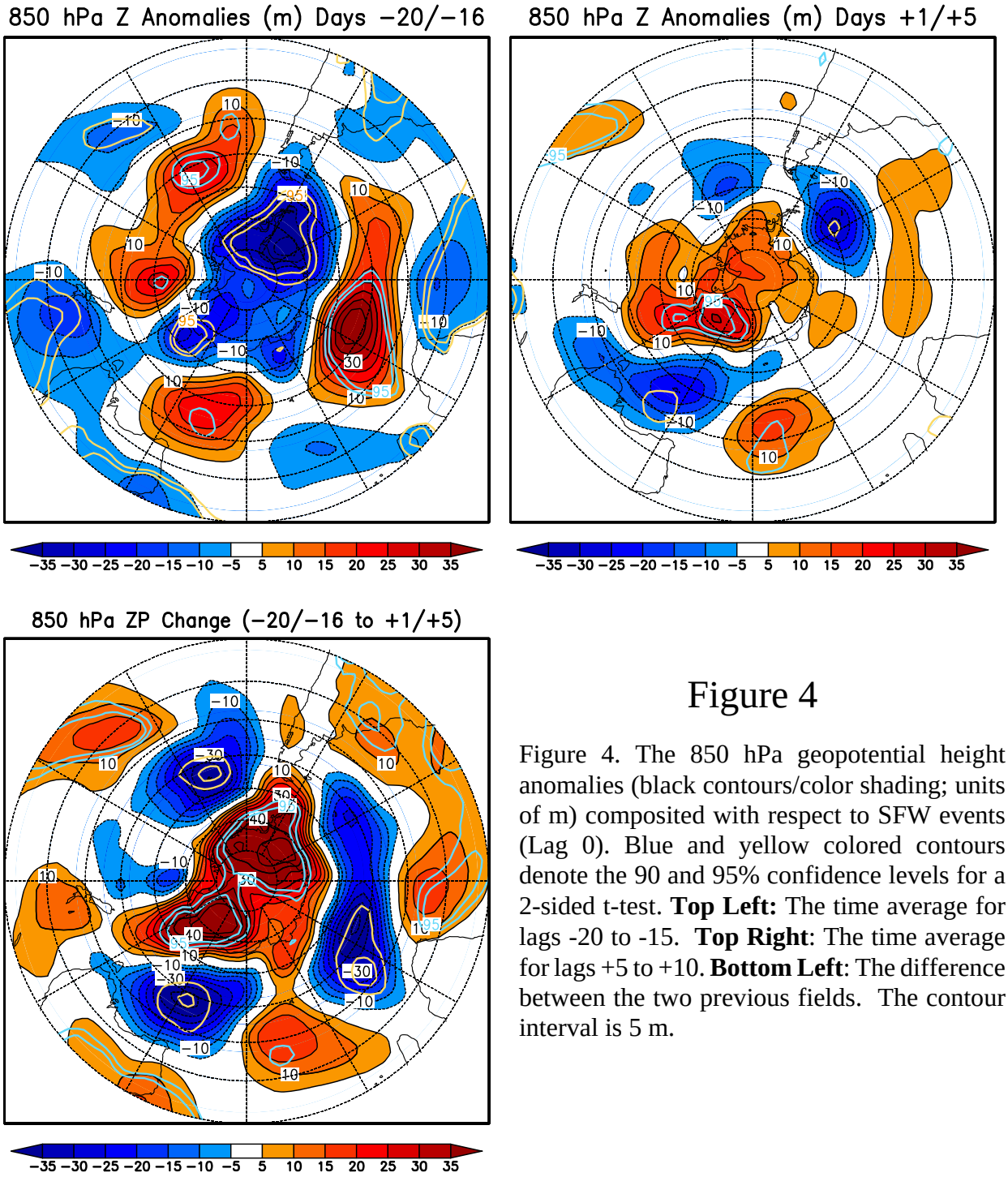

Figure 4

Figure 4. The 850 hPa geopotential height anomalies (black contours/color shading; units of m) composited with respect to SFW events (Lag 0). Blue and yellow colored contours denote the 90 and 95% confidence levels for a 2-sided t-test. **Top Left:** The time average for lags -20 to -15. **Top Right**: The time average for lags +5 to +10. **Bottom Left**: The difference between the two previous fields. The contour interval is 5 m.